

## Frequency-Dependent Characterization of Bulk and Ceramic Bypass Capacitors

Istvan Novak, Jason R. Miller  
SUN Microsystems, Inc.

One Network Drive, Burlington, MA 01803  
tel: (781) 442 0340, fax: (781) 442 0402

e-mail: istvan.novak@sun.com, jason.r.miller@sun.com

### Abstract:

*Power distribution networks use various kinds of capacitors to create the required impedance profile and to suppress noise. The simple model of bypass capacitors is a series R-L-C network with frequency independent parameters. The paper gives measured data for various bulk and ceramic capacitors, showing the extraction procedure and frequency dependent data of all three parameters. Various physical contributors to the frequency dependencies are identified. From low frequencies up to SRF, capacitance can drop as much as 60%. Inductance should be measured in a small PCB fixture with planes, vias and pads representing the intended application. The added inductance due to the capacitor body is shown to be fairly independent of via length connecting to the nearest planes.*

### I. Introduction

Often times the *power distribution network* (PDN) is designed and validated in the frequency domain. The most frequently used elements in PDS are the bypass capacitors. They range from polymer and electrolytic capacitors with thousands of microfarad capacitance to ceramic capacitors in the pF capacitance range. The typical model is a series R-L-C network, creating a *series resonance frequency* (SRF), where the part shows its *equivalent series resistance* (ESR). Beyond the SRF, the impedance is dominated by inductance, usually called as *equivalent series inductance* (ESL). In first approximation, all three parameters are independent of frequency. Upon closer inspection, these parameters all depend on frequency to various degrees and for different reasons. Moreover, some of the parameters show a frequency dependence intermingled with a dependence upon the application geometry. In this paper we give measurement data on different bypass capacitors, based on measurement and extraction procedures detailed in [1]. Effects of bias voltage and temperature are not included in this study.

### II. Limitations of frequency independent models

To illustrate the frequency dependency of parameters, we first take the measured impedance profile of a 0508-size 4.7uF two-terminal bypass capacitor as an example. The measured part does not have the lowest ESR available today, neither has it the highest capacitance in its case size, and it did not have the most aggressive mounting geometry. The part was mounted on a small piece of multilayer *printed circuit board* (PCB), and its impedance was measured on the planes using a close-by pair of vias. The test fixture had 1"x0.14" plane shapes and pads with two vias per pad. The measured impedance profile is shown in Figure 1. The impedance was measured over the 100 Hz - 1.8 GHz frequency range with two different instruments, covering the 100 Hz - 10 MHz and 100 kHz - 1800 MHz frequency ranges. The impedance plot shows the SRF at 2.65 MHz and the *parallel resonance frequency* (PRF) between the capacitor's inductance and the plane capacitance at 682 MHz. At SRF, the impedance reading is 6.48 mOhms, which may be used as the ESR estimate. From the 100 Hz impedance point, the capacitance was found to be  $C_0 = 4.94 \mu\text{F}$ . Assuming that at SRF  $C_0$  resonates with ESL, the  $L(\text{SRF})$  estimate is 729 pH. The plane capacitance of the small test fixture was measured as  $C_p = 115 \text{ pF}$ . Assuming that at PRF ESL resonates with  $C_p$ , the  $L(\text{PRF})$  estimate becomes 474 pH. The slopes on the Bode plot appear to be linear, suggesting frequency independent capacitance and inductance. By extracting the  $C(f)$ ,  $L(f)$ , and  $R(f)$  functions, they reveal considerable frequency dependency. Figures 2 and 3 show these extracted parameters. From these curves,  $C(100\text{Hz}) = 4.94 \mu\text{F}$ ,  $C(\text{SRF}) = 4.0 \mu\text{F}$  or a -19% change;  $L(\text{SRF}) = 870 \text{ pH}$ ;  $L(\text{PRF}) = 470 \text{ pH}$ , or a -46% change. Later we show that C and L can vary significantly more, depending on the part and its mounting. Figure 4 shows the percentage error of impedance magnitude between the measured (Figure 1) and estimated curves with four combinations of constant C, L and R values.

### III. Procedure to extract frequency-dependent parameters

It is known [2] that above SRF, the current loop inside the capacitor changes and therefore as frequency goes up resistance increases and inductance decreases. The magnitude and slope of change depends on  $\text{ESR}(\text{SRF})$  and on the relative dimensions of the capacitor body, pads, vias and closest plane(s). Because the  $R(f)$  and  $L(f)$  functions also depend on the application geometry, it is important to measure the part in a fixture, with pad, via and plane geometries

being similar to the actual usage. The measured  $Z_m$  impedance will reflect both the device under test and the fixture. To determine the DUT parameters, we use the equivalent circuit of Fig. 6e of [1].

**Capacitance:** Using a small fixture, we make sure that its static plane capacitance is much smaller than the capacitance of the DUT. The fixture for taking data for Figure 1 had a  $C_p = 115$  pF capacitance, allowing us to measure DUT capacitances as low as 10nF without compensating for fixture capacitance. We therefore assume that below SRF, the imaginary part of the measured impedance,  $\text{Im}\{Z_m\}$  comes from DUT capacitance. In reality, anywhere below PRF,  $\text{Im}\{Z_m\}$  is the sum of the capacitive and inductive reactances. Far below or above SRF, the capacitance or inductance dominates and the other can be neglected. Close to SRF, assuming that  $L(f)$  does not jump suddenly, we can obtain a corrected  $C(f)$  estimate (eq.8 in [1]), which extends the validity of  $C(f)$  extraction to SRF. Figure 5 shows  $C(f)$  from Figure 2 on an extended scale, with and without applying correction for  $L(\text{SRF})$ . Below SRF, this frequency dependency is believed to come from  $\epsilon_r$  variations of the ceramic material.

**Inductance:** Above SRF and below PRF, the imaginary part of  $Z_m$  is dominated by inductance. If we simply invert  $\text{Im}\{Z_m\}$  to calculate  $L(f)$ , the curve shows an increasing negative error close to SRF and increasing positive error close to PRF, see the uncorrected curve of Figure 7. Knowing the  $C_p$  fixture capacitance, and having an estimate on  $C(\text{SRF})$ , we can compensate for both resonances, by applying Eq. 12 of [1]. The corrected curve in Figure 7 is valid over almost three decades of frequency. The curve represents the entire loop formed by the pads, vias, planes and the capacitor body itself. We can also obtain the added inductance of the capacitor body, beyond the inductance of the shorted pads. This is a good indication of the high-frequency ‘goodness’ of the capacitor. The trace of added inductance in Figure 7 shows that this particular 0508 capacitor body, together with the given pads and vias, created an extra inductance, varying from 300 pH at SRF to about 50 pH at PRF, a six-to-one range.

**Resistance:** As opposed to capacitance and inductance,  $\text{Real}\{Z_m\}$  is not the sum of parameters changing with frequency in opposite ways. However, it is still the sum of the series resistance of the fixture,  $R_{fx}$ , and the series and parallel losses  $R_s$  and  $R_p$  of the capacitor. In the curve of Figure 3, the  $R_p$  dielectric loss dominates the slope up to about 100kHz. Above 100kHz, the  $R_s + R_{fx}$  conductive loss dominates. Figure 8 shows the deembedding stages: first the shorted fixture is measured, and its  $R_{fx}(f)$  curve is plotted. The deembedded resistance of DUT becomes  $\text{Real}\{Z_m(f)\} - R_{fx}(f)$ . At SRF, the deembedded ESR(SRF) resistance of DUT is 2.70 mOhms. Note: before deembedding, the ESR(SRF) estimate was 6.48 mOhms.

#### IV. Data of various bulk and ceramic capacitors

Figure 9 shows the normalized  $C(f)$  curves of seven bulk capacitors, labeled A through G. A and B are 1200uF and 1000uF low-ESR radial bulk capacitors, C and D are 330uF and 390uF D-size polymer capacitors, E, F and G are 100uF X5R, 1uF X7R 0508 and 0.1uF X7R 0402 ceramic capacitors. The curves are shown up to SRF. Figure 10 shows the inductance together with fixture for the four bulk capacitors. Parts A and B, as well as C and D shared the same fixture, respectively. Note the large range of inductances and the strong frequency dependence of D. C is face-down, low-inductance part [3]. Figure 11 shows the inductance, together with the test fixture, for the three ceramic capacitors. The 0402-size 0.1uF part (G) was measured with the same via diameter and pad arrangements with two via lengths: 130 mils and 5 mils. Curve for the 100uF part was measured only up to 10 MHz. Figure 12 gives the added inductance of one bulk capacitor (part A, 1200uF radial) and one ceramic capacitor (part G, 0.1uF 0402). The two test fixtures had mirrored pads on both top and bottom, connected to the planes, which were closer to one side. The via lengths for part A were 52-mil and 6-mil, for part G 130-mil and 5-mil. Note that the added inductance of the part is fairly independent of the via length, and therefore it is a good measure of the ‘goodness’ of capacitor.

#### Acknowledgement:

The authors wish to thank Deborah Foltz, Merle Tetreault, Eric Blomberg, all of SUN Microsystems for their contributions to the test fixtures.

#### References:

- [1] I. Novak, “Frequency-Domain Power-Distribution Measurements – An Overview,” HP-TF1 TecForum, DesignCon East, June 23, 2003, Boston, MA
- [2] L.D.Smith, D.Hockanson, K.Kothari, “A Transmission-Line Model for Ceramic Capacitors for CAD Tools Based on Measured Parameters,” Proc 52<sup>nd</sup> Electronic Components & Technology Conference, San Diego, CA., May 2002, pp.331-336
- [3] Michihiro Shirashige, Keiji Oka, Kazuto Okada, “New Structure 1608 Size Chip Tantalum Capacitor - 6.3WV 1uF -with Face-down Terminals for Fillet-less Surface Mounting,” Proc 51st Electronic Components & Technology Conference, Orlando, FL., May 2001

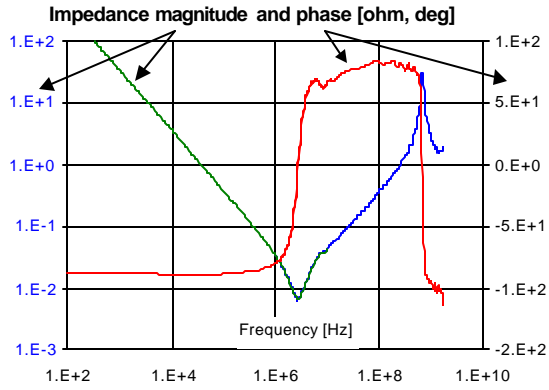


Figure 1: Impedance magnitude and phase of a 4.7uF 0508 ceramic capacitor on a small test board.

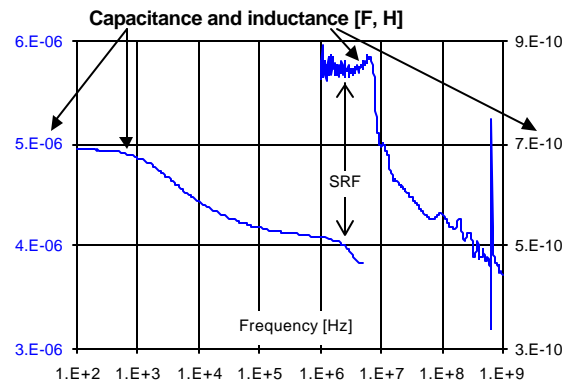


Figure 2: C(f) and L(f) parameters extracted from data of Figure 1. Note the variations with frequency.

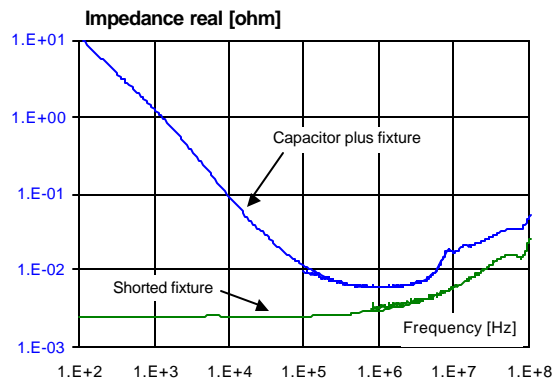


Figure 3: R(f) from data of Figure 1 (Capacitor plus fixture) and shorted fixture without capacitor.

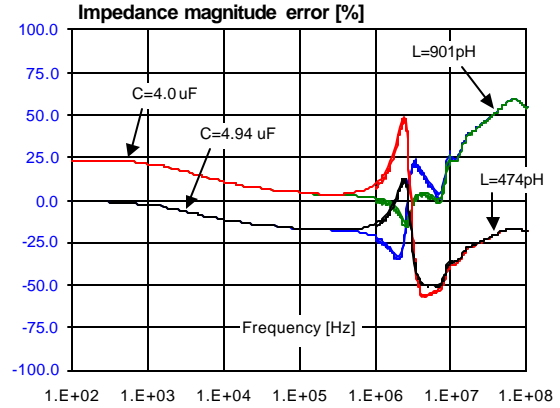


Figure 4: Percentage error of estimated impedance magnitude with constant C, L and R= 6.48 mOhms.

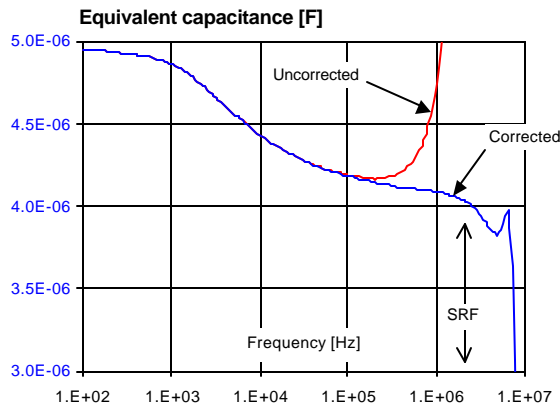


Figure 5: C(f) extracted from impedance of Figure 1, with and without correcting for SRF.

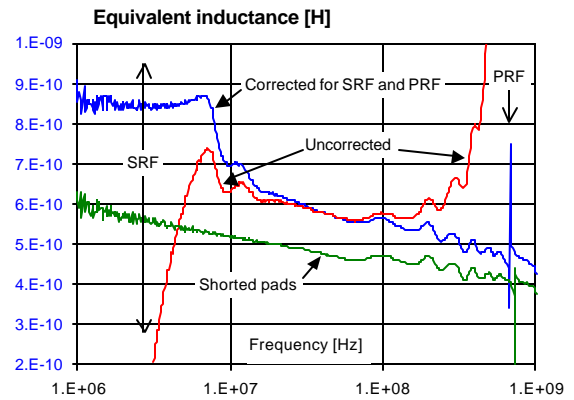


Figure 6: L(f) extracted from impedance of Figure 1, with and without correcting for SRF and PRF. Shorted pad's inductance is also shown

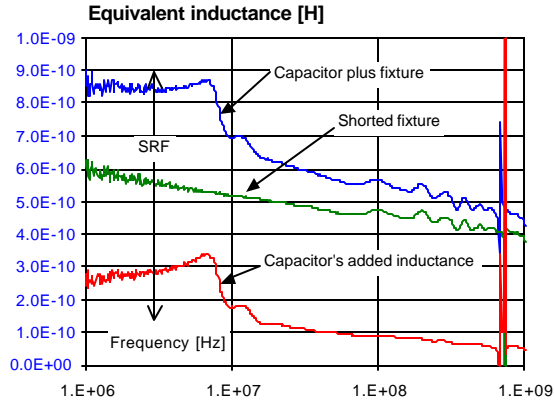


Figure 7: Components of  $L(f)$ , extracted from data of Figure 1. Spikes at 680MHz are due to PRF.

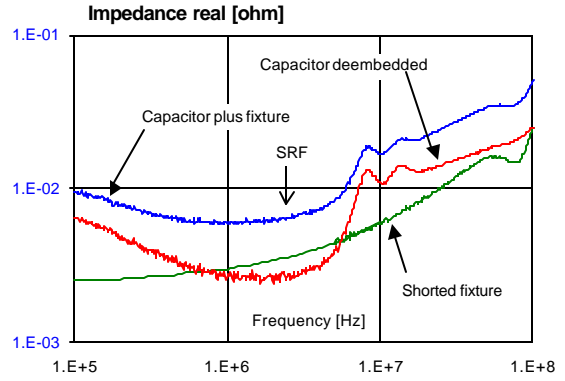


Figure 8: Deembedded real part of impedance from capacitor data from Figure 1.

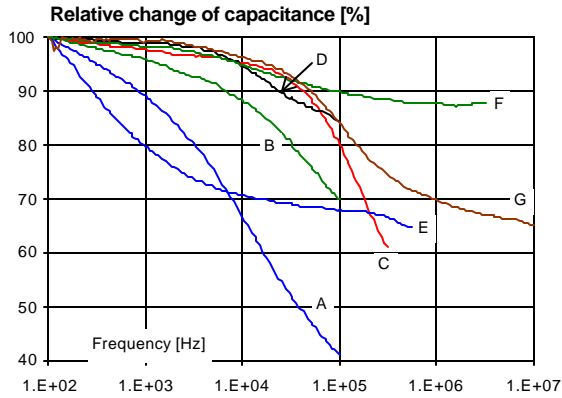


Figure 9: Normalized  $C(f)$  curves for two radial bulks (A, B), two D-size bulks (C, D) and three ceramic capacitors (E, F, G).

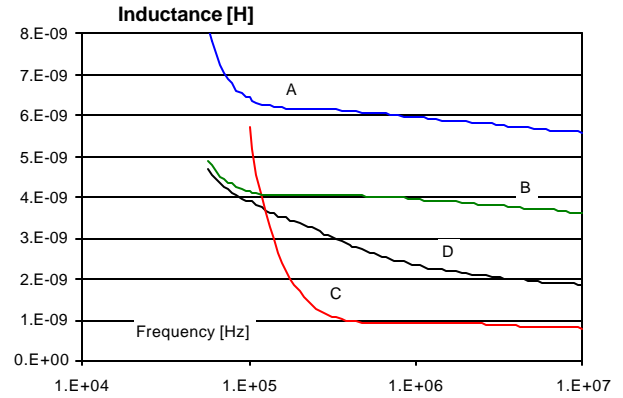


Figure 10:  $L(f)$  curves of the four bulk capacitors from Figure 9. Parts A, B and C, D had the same fixture, respectively.

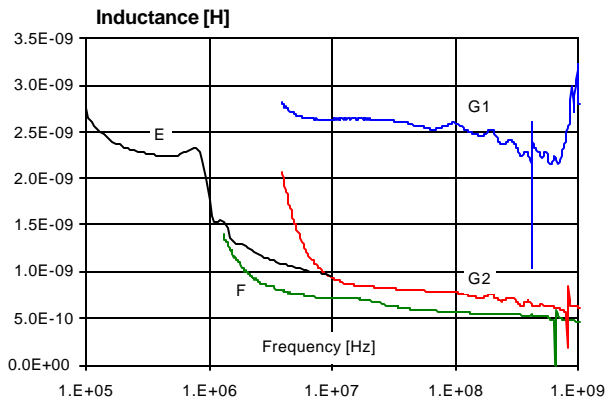


Figure 11:  $L(f)$  curves for the ceramic parts from Figure 9. G1 and G2 were measured with 130-mil and 5-mil long vias, respectively, with same via spacing and pads.

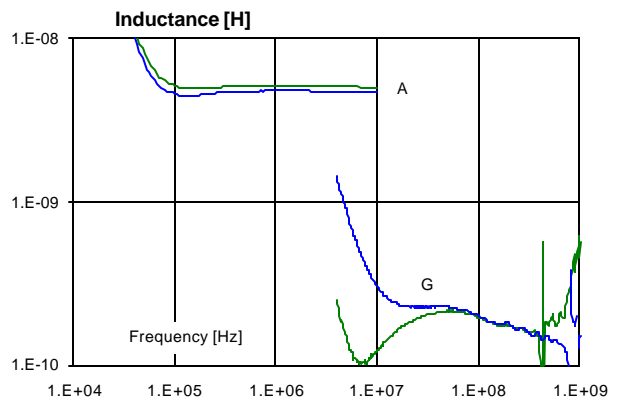


Figure 12: Added inductance of parts A and G with different lengths of vias: 52-mil and 6-mil for A, and 130-mil and 5-mil for G, with same via spacing and pads.